JCTC Journal of Chemical Theory and Computation

Article

pubs.acs.org/JCTC

Excited-State Geometries of Heteroaromatic Compounds: A Comparative TD-DFT and SAC-CI Study

Diane Bousquet,[†] Ryoichi Fukuda,[‡,#] Phornphimon Maitarad,[‡] Denis Jacquemin,[§,∥] Ilaria Ciofini,[†] Carlo Adamo,*[,†,∥] and Masahiro Ehara*[,‡,#]

[†]LECIME, Laboratoire d'Electrochimie, Chimie des Interfaces et Modélisation pour l'Energie, UMR 7575 CNRS, Ecole Nationale Supérieure de Chimie de Paris − Chimie ParisTech, 11 rue P. et M. Curie, 75231 Paris Cedex 05, France

[‡]Institute for Molecular Science and Research Center for Computational Science, 38 Nishigo-naka, Myodaiji, Okazaki, 444-8585, Japan

[§]CEISAM, UMR CNRS 6230, BP 92208, Université de Nantes, 2, Rue de la Houssinière, 44322 Nantes, France

[∥]Institut Universitaire de France, 103 Boulevard Saint Michel, F-75005 Paris, France

[#]Elements Strategy Initiative for Catalysts and Batteries (ESICB), Kyoto University Katsura, Kyoto 615-8510, Japan

Supporting Information

ABSTRACT: The structures of low-lying singlet excited states of nine π-conjugated heteroaromatic compounds have been investigated by the symmetry-adapted cluster-configuration interaction (SAC-CI) method and the time-dependent density functional theory (TDDFT) using the PBE0 functional (TD-PBE0). In particular, the geometry relaxation in some $\pi\pi^*$ and $n\pi^*$ excited states of furan, pyrrole, pyridine, *p*-benzoquinone, uracil, adenine, 9,10-anthraquinone, coumarin, and 1,8-naphthalimide as well as the corresponding vertical transitions, including Rydberg excited states, have been analyzed in detail. The basis set and functional dependence of the results was also examined. The SAC-CI and TD-PBE0 calculations showed reasonable agreement in both transition energies and excited-state equilibrium structures for these heteroaromatic compounds.

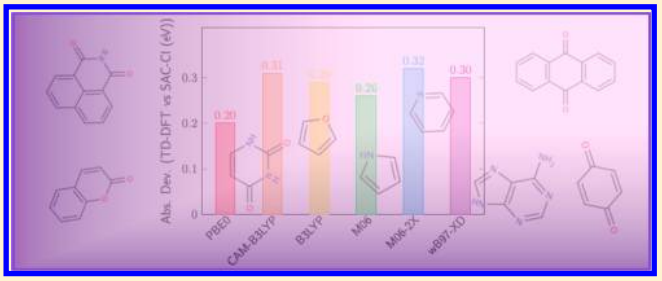

1. INTRODUCTION

Electronic properties, geometric structures, and spectroscopic constants of molecules in excited electronic states represent fundamental quantities for many functional molecules, like those involved in technological applications including light-emitting dyes or fluorescent probes. These excited states are usually characterized by a (very) short lifetime so that their full experimental characterization is very difficult if not impossible. Therefore, all information that can be brought by theory is particularly valuable not only for the rationalization of chemical phenomena (as, for instance, in photophysics or photochemistry) but also for the design (and prediction) of new photoactive systems. The development and validation of quantum chemical methods providing reliable predictions of the excited-state geometries and electronic properties is, therefore, a very active field.

Accurate theoretical spectroscopy has been achieved using various *ab initio* wave function theories, in particular, methods based on cluster expansion such as symmetry-adapted cluster−configuration interaction (SAC-CI),[1−3] coupled cluster linear response theory (CC-LRT),[4,5] and equation-of-motion coupled cluster (EOM-CC).[6,7] The multireference methods, multireference singles and doubles configuration interaction (MR-SDCI),[8,9] complete-active-space perturbation theory (CAS-PT2),[10] and multireference second-order Møller−Plesset perturbation theory (MR-MP2)[11] are particularly effective for systems where quasi-degenerate states or multielectron processes appear. Beyond the calculations of vertical transition energies, analytical energy gradients provide access to many excited-state properties, including dipoles, geometries, and vibrational frequencies as well as energy relaxation processes, and these gradients have been implemented in most of these methods. However, gradients are particularly demanding in time and computer resources so that large-scale calculations are often prohibitive, especially when, as it is often the case for many chemical applications, high-speed throughput is required.

Among all alternative computational methods, time-dependent density functional theory (TD-DFT) has emerged as the one providing an optimal ratio between accuracy and speed. A large number of benchmarks is available in the literature, and the obtained results show that functionals containing between 20 and 30% of Hartree−Fock exchange provide accurate (i.e., within about 0.2 eV) results for vertical valence excitations.[12,13] More problematic cases, such as those characterized by charge-transfer excitations, are correctly described by range-separated hybrids, albeit with larger deviations.[14] More limited are, instead, the data available for emission energies and, in particular, those concerning the structure of (lowest) excited state(s). Indeed, from one side analytical TD-DFT derivatives have been implemented only recently in commercial codes,[15] and, from the other side, the comparison with the experiments is often difficult (vertical or 0−0 transitions)

Received: February 7, 2013
Published: March 19, 2013

and requires at least the inclusion of environmental effects.[16,17] A fair assessment of excited-state structures thus requires a comparison with other theoretical methods. Performances of TD-DFT relying on several functionals in predicting excited-state structures have been previously examined with a specific focus on single and double bonds of linear conjugated systems.[18] It was demonstrated that the B3LYP[19] and PBE0[20] functionals provide results in good agreement with the CASPT2 method for both geometry and transition energy. However, the number of molecules and states considered in this first study was rather limited, and the CASPT2 results, taken from literature data, were obtained with quite compact basis sets. Therefore, in order to fill this informative gap on TD-DFT's *pros* and *cons*, a robust and effective post-Hartree−Fock reference is needed. The SAC-CI method[1−3] has been established for investigating molecular excited states via numerous applications in molecular spectroscopy, biological chemistry, material science, and surface photochemistry.[21,22] The analytical energy gradients of the method have also been formulated and implemented for the first derivatives.[23−25] SAC-CI has been used to calculate the equilibrium geometries and one-electron properties in various electronic states such as the excited, ionized, electron-attached, and high-spin states.[22,25,26] Although this approach is useful for calculating excited-state equilibrium geometries, the method has not yet been applied to large systems. The SAC-CI method makes use of a selection of operators,[27] effective for large-scale calculations. However, this approximation sometimes causes inaccuracies in the computed PESs and energy derivatives. Recently, a direct algorithm for the SAC/SAC-CI method (direct SAC-CI) has been developed,[28] and the calculation of all the necessary product operators, without any cutoff, has become possible. This method is expected to be useful and stable for the calculation of the excited-state geometries of large systems and hence can be used to provide reliable benchmarks for TD-DFT calculations.

On those bases, the geometries of some low-lying valence excited states of nine π-conjugated heteroaromatic compounds were investigated by the direct SAC-CI and TD-DFT methods. The molecule set includes furan, pyrrole, pyridine, *p*-benzoquinone, uracil, adenine, 9,10-anthraquinone, coumarin, and 1,8-naphthalimide (see Figure 1), and the target states were not limited to the lowest excited state but also included several higher ones. The results obtained with the two approaches are compared in detail, and the characteristics of the methods are addressed.

2. COMPUTATIONAL DETAILS

All *ab initio* and DFT calculations including the direct SAC-CI and TD-DFT calculations were performed using Gaussian 09 revision B01.[29] In direct SAC-CI[28] for absorption energies, two sets of calculations were performed: one with DZP basis and the other with TZP basis set augmented by diffuse functions. The first set of calculations starts from the ground-state SAC/D95(d,p)[30] optimization with MP2/D95(d,p) geometries as the initial geometry. MacroIteration of the geometry optimization was performed in this set of calculations. The obtained structures were then used to compute vertical transition energies using the D95(d,p) basis set. In these calculations, the LevelThree accuracy (energy thresholds of $\lambda_g = 1 \times 10^{-6}$ and $\lambda_e = 1 \times 10^{-7}$) was adopted for the perturbation selection. Details are given in the Supporting Information (SI). The other set of calculations starts from the ground-state SAC/6-311G(d)[31] optimizations using the geometries obtained at the B3LYP/6-311G(d) level as starting points. These calculations were followed by the SAC-CI calculations for the vertical absorption with the 6-311G(d)[31] basis augmented by Rydberg s and p functions [2s2p]. The exponents of the Rydberg functions [2s2p] were obtained by applying the multiplication factors of 1.9 and 0.85, respectively, to the original Dunning Rydberg functions.[32] The latter set of calculations was performed for furan, pyrrole, pyridine, uracil, and adenine. For *p*-benzoquinone, SAC-CI/6-311++G(2d,2p) was done.

The geometry optimizations of some low-lying excited states were also carried out by the SAC-CI analytical energy gradients. The CIS/D95(d,p) structures were used as a starting point, and the MacroIteration method was applied. The LevelThree accuracy was adopted for the perturbation selection. All the product R_1S_2 and R_2S_2 terms were included. For uracil and adenine, the C_s structure is not the local minimum in the ground state; however, the symmetry-restriction was used for the ground and excited states to avoid a conical intersection.

Concerning DFT calculations, ground-state structures were optimized using the PBE0[20] functionals and the D95(d) basis set. Vertical excitation energies were then computed at the TD-DFT level with the D95(d,p) basis set as well as with more extended 6-311++G(2d,2p) and aug-cc-pVTZ basis set.[33] Structures of the lowest excited states were also optimized, following the SAC-CI symmetry assignments and constrains. Further exploratory calculations were carried out with the B3LYP,[19] CAM-B3LYP,[34] M06,[35] M06-2X,[36] ωB97X-D[37] functionals.

3. RESULTS AND DISCUSSION

As mentioned in the Introduction a set of selected organic molecules, represented in Figure 1, has been considered in the

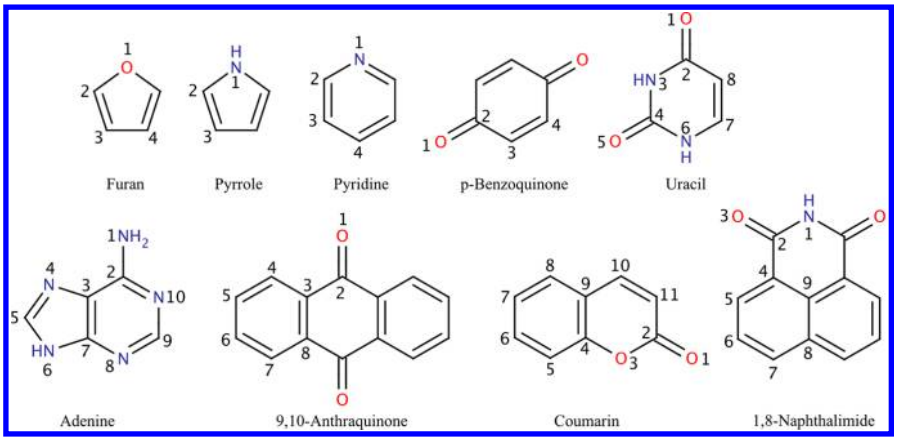

Figure 1. Molecular structures and atoms numbering of the heteroaromatic compounds studied in the present work.

Table 1. Vertical Excitation Energies (ΔE, eV) and Oscillator Strength (f) Computed for Furan, Pyrrole, and Pyridine (Absorption Spectra) at Both TD-PBE0 and SAC-CI Levels

TD-DFT (PBE0)								SAC-CI						
D95(d,p)		6-311++G(2d,2p)			*aug*-cc-pVTZ			D95(d,p)		6-311G(d)+Ryd.[2s2p]			expt[a]	
	ΔE		ΔE	f		ΔE	f		ΔE		ΔE	f	ΔE	character
Furan														
B_2	6.35	A_2	5.82	-	A_2	5.75	-	B_2	6.84	A_2	5.82	-	5.91	3s
A_1	6.86	B_2	6.10	0.167	B_2	6.06	0.168	A_1	6.93	B_2	6.36	0.153	6.04	V
A_2	8.68	B_1	6.29	0.032	B_1	6.21	0.029	A_2	8.96	B_1	6.34	0.036	6.47	$3p_y$
B_1	8.83	A_2	6.49	-	A_2	6.38	-	B_1	9.36	A_2	6.51	-	6.61	$3p_z$
B_1	9.11	B_1	6.97	0.000	B_1	6.84	0.000			B_2	6.76	0.024	6.75	$3p_x$
Pyrrole														
B_2	6.56	A_2	5.01	-	A_2	4.98	-	A_1	6.63	A_2	4.95	-	≈ 5.22	3s
A_1	6.67	B_1	5.76	0.028	B_1	5.69	0.027	B_2	6.90	B_1	5.63	0.017	≈ 5.7	$3p_y$
A_2	7.22	A_2	5.79	-	A_2	5.70	-	A_2	7.63	A_2	5.68	-		$3p_z$
B_1	8.08	B_1	5.90	0.002	B_1	5.87	0.001	B_1	8.33	B_1	5.76	0.013		3s'
B_2	8.35	A_2	6.38	0.000	B_2	6.07	0.169			B_2	5.83	0.066	≈ 5.86	$3p_x$
Pyridine														
B_1	4.87	B_1	4.86	0.004	B_1	4.82	0.004	B_1	5.11	B_1	4.90	0.006	4.44, 4.59	n-π^*
A_2	5.19	A_2	5.22	-	A_2	5.19	-	B_2	5.20	B_2	5.07	0.031	4.99	$\pi-\pi^*$
B_2	5.58	B_2	5.51	0.043	B_2	5.51	0.043	A_2	5.50	A_2	5.39	-		3s
A_1	6.41	A_1	6.31	0.017	A_1	6.30	0.016	A_1	6.57	A_1	6.31	0.004	6.38	$\pi-\pi^*$
B_2	7.43	A_1	6.61	0.002	A_1	6.31	0.002			A_2	6.48	-		n-π^*

[a]References 38−46 and references therein.

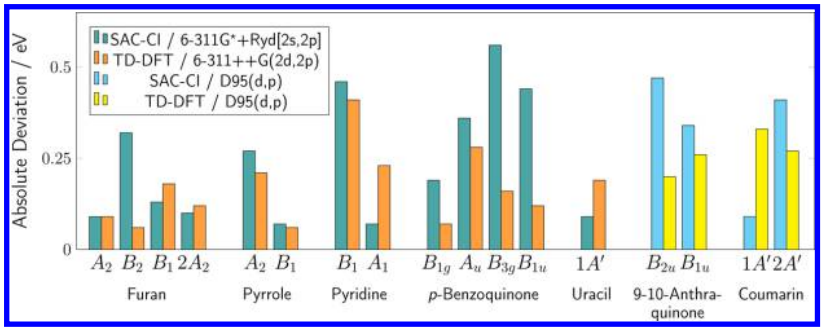

Figure 2. Comparison between SAC-CI and TD-DFT/PBE0 absorption energies for selected states.

present work. The first part of the study consisted in the evaluation of the absorption spectra at both SAC-CI and TD-DFT levels, the latter being limited to the PBE0 functional. This choice was dictated by two main reasons: i) many studies have shown that this functional can be considered as the reference for TD-DFT excited-state calculations and, particularly for vertical absorption;[12] ii) the purpose of this analysis of the results is to separate the SAC-CI/TD-DFT comparison from the functional effects. In the following, we deal with the effect of the exchange-correlation functional on the emission energies and optimized excited-state structures.

3.1. Absorption Spectra. Albeit a large number of benchmarks concerning absorption spectra are available in the literature (see for instance refs 12−14), vertical transition energies were first analyzed with the double aim to verify the coherence on the nature of the low-lying exited states for the two considered methods (TD-DFT and SAC-CI) and their relative performances. The calculated absorption energies and oscillator strengths of five low-lying singlet excited states of furan, pyrrole, and pyridine are listed in Table 1 together with the experimental values,[38−46] while selected results are shown in Figure 2. In this part, two basis sets have been considered, namely the D95(d,p), which is suitable only for valence excited states and the larger 6-311++G(2d,2p) able to describe both valence and Rydberg excited states.[47] TD-PBE0 calculations have been also carried out with the larger *aug*-cc-pVTZ basis, in order to ensure the convergence of the obtained results.

The low-lying excited states of furan and pyrrole are mostly characterized as Rydberg excited states corresponding to π-3s and π-3p transitions.[38−40,44,45] For these Rydberg states, the PBE0/6-311G++(2d,2p) and SAC-CI/6-311G(d)+[2s2p] calculations provide similar excitation energies that nicely fit the experimental values. For instance, the calculated transition energy of the lowest A_2 state of furan is computed to be 5.82 eV at both levels of theory, in very good agreement with the experimental value of 5.91 eV. For the valence $\pi\pi^*$ excited state of furan, PBE0 predicts a satisfactory transition energy of 6.10 eV compared to the experimental value of 6.04 eV, whereas SAC-CI yields 6.36 eV. Similar results were obtained in a previous SAC-CI work using a larger basis set.[45] Therefore, even if the convergence with respect to higher angular momentum in the basis set is slower in wave function based methods than in DFT, the 6-311G(d)+[2s2p] provides converged SAC-CI values. The vibronic coupling effects may exist for this discrepancy.[48] The splitting of the molecular field, namely, the energy differences among 3p transitions, is computed to be larger in PBE0 than in SAC-CI.

dx.doi.org/10.1021/ct400097b | J. Chem. Theory Comput. 2013, 9, 2368−2379

Table 2. Vertical Excitation Energies (ΔE, eV) and Oscillator Strength (f) Computed for *p*-Benzoquinone, Uracil, and Adenine (Absorption Spectra) at Both TD-PBE0 and SAC-CI Levels[g]

TD-DFT (PBE0)							SAC-CI						
D95(d,p)		6-311++G(2d,2p)			*aug*-cc-pVTZ		D95(d,p)		6-311++G(2d,2p)/6-311G(d)+Ryd.[2s2p]			expt	
	ΔE		ΔE	f	ΔE	f		ΔE		ΔE	f	ΔE	character
p-Benzoquinone													
B_{1g}	2.55	B_{1g}	2.56	-	2.55	-	B_{1g}	2.94	B_{1g}	2.68	-	2.49[a,b]	n_g^--π_g^-*
A_u	2.79	A_u	2.80	0.000	2.79	0.000	A_u	3.11	A_u	2.88	0.000	2.52[a]; 2.48[b]	n_g^+-π_g^-*
B_{3g}	3.98	B_{3g}	3.92	-	3.92	-	B_{3g}	4.92	B_{3g}	4.63	-	4.07[a]; 4.4[c];4.6[d]	π_g^+-π_g^-
B_{1u}	5.06	B_{1u}	5.00	0.335	5.00	0.335	B_{1u}	5.89	B_{1u}	5.56	0.340	5.12[a]; 5.1[c]; 5.4[d]	π_u^+-π_g^-
B_{3u}	5.59	B_{3u}	5.57	0.001	5.54	0.001	B_{3u}	6.24	B_{3u}	5.99	0.001		
Uracil													
A″	4.82	A″	4.80	0.000	4.78	0.000	A″	4.86	A″	4.66	0.000		n-π*
A′	5.41	A′	5.27	0.137	5.26	0.133	A′	5.54	A′	5.17	0.240	5.08[e]	π–π*
A″	6.01	A″	5.96	0.002	5.94	0.001	A″	6.31	A″	5.55	0.003		
A′	6.15	A″	5.97	0.000	5.95	0.001	A′	6.59	A″	6.09	0.000		
A″	6.46	A′	6.08	0.037	6.07	0.034	A′	7.14	A′	6.37	0.056	6.05[e]	π–π*
A′	6.83	A″	6.37	0.000	6.37	0.001			A″	6.51	0.012		
A″	6.93	A′	6.56	0.120	6.56	0.108			A″	6.56	0.005		
A′	7.80	A′	6.74	0.036	6.69	0.042			A′	6.62	0.108	6.63[e]	
A″	7.93	A″	6.85	0.000	6.83	0.008			A′	6.64	0.127		
A′	8.56	A″	6.89	0.008	6.84	0.000			A″	7.39	0.005		
Adenine													
A″	5.14	A′	5.13	0.223	5.12	0.224	A″	5.05	A′	4.93	0.254	4.59[f]	π–π*
A′	5.23	A″	5.14	0.001	5.11	0.000	A′	5.07	A′	5.08	0.109	4.77[f]	π–π*
A′	5.47	A′	5.36	0.031	5.35	0.030	A′	5.29	A″	5.16	0.003	5.27[f]	n-π*
A″	5.78	A″	5.49	0.007	5.43	0.007	A″	5.71	A″	5.47	0.000		
A″	6.11	A″	5.74	0.000	5.69	0.000			A″	5.50	0.001		

[a]Reference 49. (0–0 transition). [b]Reference 51. (0–0 transition). [c]Reference 52. (Band maxima). [d]Reference 50. (Band maxima). [e]Reference 53. [f]Reference 54. [g]In SAC-CI, 6-311++G(2d,2p) was used for *p*-benzoquinone and 6-311G(d)+Ryd.[2s2p] was used for uracil and adenine.

Table 3. Vertical Excitation Energies (ΔE, eV) and Oscillator Strength (f) Computed for 9,10-Anthraquinone, Coumarin, and 1,8-Naphthalimide (Absorption Spectra) at Both TD-PBE0 and SAC-CI Levels

TD-DFT (PBE0)					SAC-CI				
D95(d,p)		6-311++G(2d,2p)			D95(d,p)			expt	
	ΔE		ΔE	f		ΔE	f	ΔE	character
9,10-Anthraquinone									
B_{1g}	3.06	B_{1g}	3.05	-	B_{1g}	3.12	-		
A_u	3.33	A_u	3.33	0.000	A_u	3.36	-		
B_{3g}	3.89	B_{3g}	3.84	-	B_{3g}	4.52	-		
B_{2u}	4.03	B_{2u}	3.97	0.111	B_{2u}	4.30	0.117	~3.83[a]	
A_g	4.04	A_g	3.99	-	A_g	4.29	-		
B_{1u}	4.70	B_{1u}	4.65	0.172	B_{1u}	5.30	0.267	~4.93[a]	
Coumarin									
A′	4.32	A′	4.28	0.130	A′	4.08	0.091	3.99[b]	π–π*
A″	4.59	A″	4.69	0.000	A″	4.52	0.000		
A′	4.80	A′	4.74	0.154	A′	4.94	0.173	4.53[b]	π–π*
A′	5.58	A′	5.48	0.030	A′	5.83	0.035		
A′	6.00	A′	5.89	0.166	A′	6.15	0.539		
1,8-Naphthalimide									
A_1	3.89	A_1	3.83	0.175	B_2	3.95	0.029	3.60, 3.76[c]	n-π*
B_1	3.91	B_1	3.91	0.000	B_1	4.13	0.000		
B_2	4.18	B_2	4.15	0.029	A_1	4.16	0.274		
A_2	4.43	A_2	4.43	-	A_2	4.58	-		
B_2	4.85	B_2	4.82	0.006					

[a]In polyethylene, ref 62. [b]In 10% methanol, ref 63. [c]In cyclohexane, ref 64.

The excited states of pyridine, including both nπ* and $\pi\pi$* transitions, in the low energy region[46] are coherently described by both theoretical approaches, even if a large error (0.3–0.4 eV) is found for the lowest nπ* transition. Let us also underline the relative order of the A_2 and B_2 states, PBE0 providing a higher transition energy for the B_2 state than SAC-CI.

dx.doi.org/10.1021/ct400097b | J. Chem. Theory Comput. 2013, 9, 2368–2379

The results obtained for biologically relevant molecules, *p*-benzoquinone, uracil, and adenine, are collected in Table 2 together with experimental values.[49−54] The excited states of these molecules have already been intensively studied in many other theoretical works, using, for example, CASPT2,[55,56] SAC-CI,[57] or EOM-CC methods.[58] Here, we focused on the low-lying valence excited states except for uracil, even if other theoretical calculations were performed up to higher energy regions.[59]

For *p*-benzoquinone, there are four low-lying relevant valence excited states characterized as the transitions to π_g^-* orbitals. The B_{1g} and A_u states are attributed to the transitions from n_g^- and n_u^+ orbitals, respectively, and the B_{3g} and B_{1u} states are the transitions from π_g^+ and π_g^-orbitals, respectively.[57] Again, PBE0 and SAC-CI reasonably match the experiment for the first two states. The PBE0 gave excellent results for two higher $\pi\pi$* excited states, while the SAC-CI results for these states deviated largely from experimental values. The previous SAC-CI results obtained with the extended basis set, 4.52 and 5.47 eV for these states,[57] indicate that these deviations would be partly attributed to the quality of the basis set.

In the UV−vis spectrum of uracil, intense absorption peaks were observed at about 5.08, 6.05(shoulder), and 6.63 eV.[53] Therefore, the calculations were extended to the higher energy region for uracil in the present calculations, in contrast with previous EOM-CC calculations.[58] The vertical transitions with large oscillator strengths were obtained at 5.17, 6.37, 6.62, and 6.64 eV in A′ symmetry at the SAC-CI/6-311G*+[2s2p] level. These transitions reproduce well the experimental UV−vis spectrum and are in good agreement with the TD-PBE0 results.

Strong absorption peaks were observed at 4.59 and 4.77 eV for adenine.[54,60,61] Accordingly, the $\pi-\pi$* (A′) excited states were calculated at 4.93 and 5.08 eV by SAC-CI. The n-π* (A″) state was obtained at 5.16 eV (versus an experimental value of 5.26 eV), and diffuse states were also calculated at 5.47 and 5.50 eV. For this nucleobase, the PBE0 energies are slightly higher than the experimental values (see Table 2).

Finally, the SAC-CI and PBE0 results of three important fluorescent dyes, 9,10-anthraquinone, coumarin, and 1,8-naphthalimide, are summarized in Table 3 together with experimental values.[62−64] The photophysical properties (i.e. absorption and fluorescence) of these dyes and their derivatives have been intensively investigated in view of solvatochromism, particularly at TDDFT.[65−69] In the present work, the low-lying five excited states were examined only in the gas phase, and, since they are mostly valence states in nature, they are correctly described by the D95(d,p) basis.

In the absorption spectrum of 9,10-anthraquinone, the most intense peaks were observed at 4.46 and 4.97 eV in a polyethylene sheet.[62] The SAC-CI and PBE0 results with D95(d,p) are in good agreement with the experiments, the deviations not exceeding 0.3 eV. Among these low-lying states, the $1B_{2u}$ and $1B_{1u}$ states are the optically active ones, and the SAC-CI computes transition energies of 4.30 and 5.30 eV for these two states, respectively. The PBE0 results are less basis set dependent, and the first state appears at 4.03 eV.

For coumarin, the prominent peaks were calculated at 4.28 (1A′), 4.74 (2A′), and 5.89 (3A′) eV with respective oscillator strengths of 0.130, 0.154, and 0.166 at the PBE0/6-311++G(2d,2p) level. The experimental values of the first two prominent peaks are 3.99 and 4.53 eV (311 and 274 nm).[63] For 1,8-naphthalimide, the $1A_1$ and $1B_2$ states which are characterized as $\pi-\pi$* transitions, were calculated at 3.83 and 4.15 eV, respectively, with oscillator strengths of 0.175 and 0.029 with the D95(d,p) basis set. The lower state was observed at 3.60 and 3.76 eV in cyclohexane.[64] The other low-lying states, $1B_1$, $1A_2$, and $1B_2$ correspond to n-π* transitions.

Overall, TD-DFT shows a smaller dependency upon the basis set than SAC-CI, the compact D95(d,p) providing values within 0.2 eV or less than larger basis sets. Such a behavior was already pointed out in previous literature.[70] A more detailed analysis on the basis set dependence of the results by PBE0 can be found in the SI. The results show a similar trend with respect to what was discussed above. In summary, a general good agreement has been found between SAC-CI and TD-PBE0 with deviations ranging between 0.00 and 0.59 eV for the lowest valence excitations.

3.2. Emission Energies. Initially, full structural optimizations of the low-lying excited states for all nine molecules were performed with the SAC-CI and TD-PBE0 methods using the D95(d) basis set. The obtained results, including the main geometrical parameters and emission energies, are reported in Tables 4−9 with available experimental fluorescence energies.[69,71−74]

Table 4. Geometrical Parameters (Å) and Emission Energies (ΔE, eV) Computed at the TD-PBE0/D95(d) and SAC-CI/D95(d,p) Levels for the Valence Excited States of Furan, Pyrrole, and Pyridine

	Furan						
	ground	$1B_2$		$1A_1$		1A″	
	SAC	SAC-CI	PBE0	SAC-CI	PBE0	SAC-CI	PBE0
ΔE	-	5.97	5.44	6.16	6.30	4.60	2.86
O_1-C_2	1.364	1.397	1.401	1.363	1.367	1.393	1.394
C_2-C_3	1.366	1.443	1.444	1.456	1.442	1.438	1.445
C_3-C_4	1.443	1.377	1.377	1.458	1.471	1.384	1.388
rmsd[a]			0.003		0.011		0.005
	Pyrrole						
	ground	$1A_1$		$1B_2$		1A″	
	SAC	SAC-CI	PBE0	SAC-CI	PBE0	SAC-CI	PBE0
ΔE	-	5.77	6.24	6.12	5.80	4.34	3.10
N_1-C_2	1.376	1.397	1.393	1.408	1.416	1.425	1.432
C_2-C_3	1.384	1.457	1.444	1.463	1.457	1.447	1.448
C_3-C_4	1.431	1.469	1.468	1.373	1.373	1.380	1.383
rmsd[a]			0.009		0.006		0.005
	Pyridine						
	ground	$1B_1$		$1B_2$		1A′	
	SAC	SAC-CI	PBE0	SAC-CI	PBE0	SAC-CI	PBE0
ΔE	-	4.12	3.97	4.82	5.27	3.57	3.97
N_1-C_2	1.342	1.365	1.352	1.374	1.366	1.366	1.353
C_2-C_3	1.399	1.382	1.380	1.433	1.430	1.383	1.380
C_3-C_4	1.398	1.430	1.429	1.432	1.427	1.428	1.429
rmsd[a]			0.008		0.006		0.008

[a]Root-mean-square deviation (rmsd) between the PBE0 and SAC-CI bond lengths.

The molecular structures and the definition of the coordinates are given in Figure 1, while the Cartesian coordinates of all the structures are given in the SI.

For the sake of straightforward comparisons, the applied state symmetries are those obtained at the SAC-CI level, and they generally match the energy order obtained for vertical absorption. However, in some cases, a symmetry lowering has been found upon full geometry convergence.

Analyzing the emission energies computed at the SAC-CI and TD-DFT levels (Figure 3), two classes of states can be defined. The first, related to emissions above 4.0 eV, that is

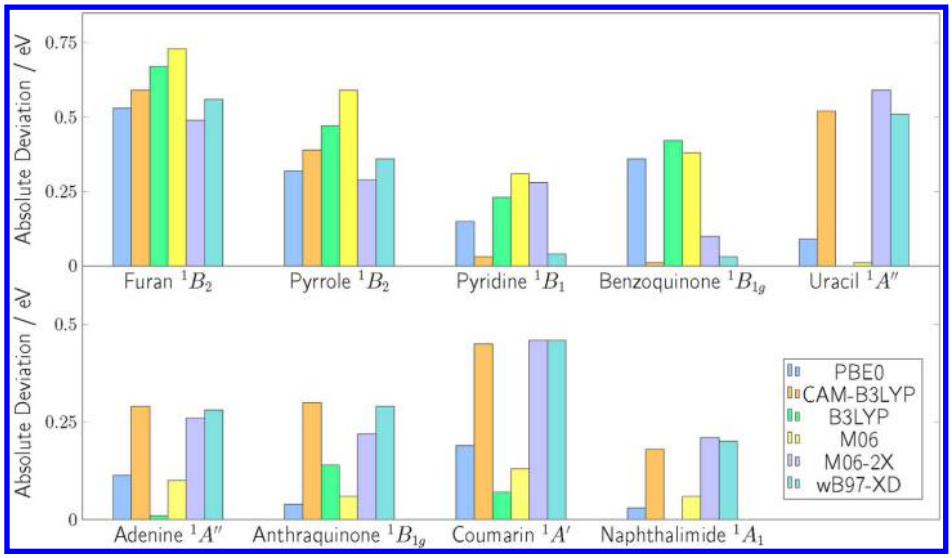

Figure 3. Effect of the selected functional on the emission energies. Comparison made with respect to the SAC-CI values.

Table 5. Geometrical Parameters (Å) and Emission Energies (ΔE, eV) Computed for the Valence Excited States of *p*-Benzoquinone at the TD-PBE0/D95(d) and SAC-CI/D95(d,p) Levels

	ground	$1B_{1g}$		$1A_u$		$1B_{1u}$		$1B_{3g}$	
	SAC	SAC-CI	PBE0	SAC-CI	PBE0	SAC-CI	PBE0	SAC-CI	PBE0
ΔE^a	-	2.70	2.34	2.59	2.27	5.41	4.62	3.98	3.00
O_1-C_2	1.224	1.256	1.250	1.272	1.286	1.266	1.250	1.252	1.250
C_2-C_3	1.491	1.468	1.461	1.451	1.443	1.466	1.467	1.451	1.449
C_3-C_4	1.346	1.355	1.355	1.370	1.374	1.386	1.401	1.412	1.418
rmsd[b]			0.006		0.009		0.022		0.003

[a]Expt (ref 71, vapor): 2.49 eV (B_{1g}). [b]rmsd between the PBE0 and SAC-CI bond lengths.

those of furan (3 states), pyrrole (3 states), pyridine (2 states), and the two highest states of *p*-benzoquinone, display typical deviations of ca. 0.5 eV between TD-DFT and SAC-CI data. The second is represented by the two lowest states of *p*-benzoquinone and the lowest state of adenine, uracil, pyridine, 9,10-anthraquinone, coumarin, and 1,8-naphthalimide, for which the deviation is 0.2 eV or less.

More in detail, the agreement of the computed emission energies for the $1A_1$ state of furan is very good (deviation 0.14 eV). In contrast, a larger deviation is observed for the $1B_2$ state, which reflects the deviation already observed in the vertical transition. For the 1A″ state, the deviation of emission energy is much larger since the nonplanarity of the equilibrium geometry is larger at PBE0 than at SAC-CI. For pyridine, the agreement between SAC-CI and TD-DFT emission energies is better than for furan and pyrrole, since the target valence excited states are located lower than the Rydberg states. The agreement in emission energies is also reasonable for the $1A_u$ and $1B_{1g}$ states of *p*-benzoquinone but not for $1B_{1u}$ and $1B_{3g}$ states. This is because diffuse functions, not included in the D95(d,p) set, are necessary for the description of these latter two states using wave function approaches.[75]

The agreement with the experimental fluorescence energies is also reasonable, and the results are compared for seven molecules in Tables 5−9. This agreement also verifies the comparison of theoretical values, though the experimental conditions are in vapor phase or in solution. Detailed comparison including the solvent effect was done for some molecules by the previous TD-DFT works.[67,69,73,76]

At this stage, it remains difficult to clearly identify the origin of the discrepancies between the results of the two methods, which does not clearly depend upon the nature of the excitations (n-π^*, $\pi-\pi^*$ or Rydberg). It could be inferred that it derived either from an intrinsic failure of TD-PBE0 or from the incomplete basis set convergence of SAC-CI. This last point is, however, cumbersome to verify due to the high computational scaling of SAC-CI with basis set.

3.3. Excited-State Structures. The excited-state geometries of furan, pyrrole, and pyridine have been intensively investigated, and the structures in lower symmetry have been found to be local minima.[77−79] For furan and pyrrole, even though the Rydberg states are located below the valence excited states, the valence excited states were optimized with D95(d,p) basis sets, and the results are reported in Table 4.

Furan was optimized imposing a C_{2v} symmetry for the valence $1A_1$ and $1B_2$ states, though these stationary points were found not to be local minima by the subsequent CIS/D95(d) vibrational analysis. The same holds for the 1A″ state in C_s symmetry. In all these states, the C_2-O_1 and C_2-C_3 bond lengths are elongated by +0.03∼+0.10 Å with respect to the SAC ground-state geometry, while those of C_3-C_4 are contracted by −0.06∼−0.07 Å. Bond alternation (change of double/single nature upon transition) occurs in the $1B_2$ and 1A″ states. The agreement between the SAC-CI and TD-PBE0 equilibrium bond lengths is very satisfactory; the root-mean-square deviations (rmsds) are 0.003, 0.011, and 0.005 Å for $1B_2$, $1A_1$, and 1A″ states, respectively.

Similarly, the equilibrium structures of the valence excited states of pyrrole were evaluated for the $1A_1$ and $1B_2$ states in C_{2v} symmetry and the 1A″ state in C_s symmetry. In the $1A_1$ state, all bond lengths are elongated with respect to the ground

state, and the change is significant for the C_2-C_3 distance (0.073 Å). In both $1B_2$ and $1A''$ states, the C−N and C_2-C_3 bond lengths are elongated and the C_3-C_4 bond length is contracted. The bond alternation occurs in the $1A''$ state.

For pyridine, two C_{2v} structures ($1B_1$ and $1B_2$ states) and one C_s structure ($1A'$ state) were optimized. The changes in geometry computed for the $1B_1$ and $1A'$ states are similar. In both states, the N_1-C_2 and C_3-C_4 bonds are elongated with respect to the ground state by ca. 0.02 and 0.03 Å, respectively, whereas the C_2-C_3 bond length contracts by −0.016 (−0.017) Å. On the other hand, all the bonds are elongated in the $1B_2$ state. The agreement between the PBE0 and SAC-CI geometries is again satisfactory; the rmsds are 0.006−0.008 Å for these structures.

The optimized structures of *p*-benzoquinone, uracil, and adenine are collected in Tables 5 and 6. The true local minima

Table 6. Geometrical Parameters (Å) and Emission Energies (Δ*E*, eV) Computed for the Valence Excited States for Uracil and Adenine Calculated at the TD-PBE0/D95(d) and SAC-CI/D95(d,p) Levels

	Uracil				
	ground	1A′		1A″	
	SAC	SAC-CI	PBE0	SAC-CI	PBE0
ΔE[a]	-	4.03	4.65	3.43	3.52
O_1-C_2	1.216	1.253	1.234	1.355	1.324
C_2-N_3	1.404	1.447	1.497	1.403	1.391
N_3-C_4	1.382	1.349	1.325	1.388	1.399
C_4-O_5	1.213	1.218	1.294	1.220	1.219
C_4-N_6	1.385	1.429	1.334	1.369	1.363
N_6-C_7	1.378	1.335	1.432	1.404	1.400
C_7-C_8	1.348	1.533	1.408	1.381	1.406
C_8-C_2	1.464	1.394	1.410	1.389	1.374
rmsd[b]		0.042		0.010	
	Adenine				
	ground	1A″		1A′	
	SAC	SAC-CI	PBE0	SAC-CI	PBE0
ΔE[c]	-	3.74	3.85	4.40	4.60
N_1-C_2	1.353	1.366	1.370	1.338	1.359
C_2-C_3	1.414	1.454	1.454	1.425	1.442
$C3-N_4$	1.385	1.359	1.341	1.366	1.340
N_4-C_5	1.310	1.312	1.324	1.320	1.357
C_5-N_6	1.375	1.400	1.405	1.385	1.390
N_6-C_7	1.375	1.368	1.366	1.401	1.393
C_7-C_3	1.390	1.405	1.413	1.445	1.433
C_7-N_8	1.342	1.326	1.322	1.293	1.304
N_8-C_9	1.329	1.397	1.382	1.436	1.408
C_9-N_{10}	1.346	1.358	1.340	1.365	1.345
$N_{10}-C_2$	1.337	1.307	1.312	1.358	1.329
rmsd[b]		0.010		0.022	

[a]Expt: 4.03 eV(ref 72), 3.97 eV (ref 73). [b]rmsd between the PBE0 and SAC-CI bond lengths. [c]Expt: 4.07−3.70 eV (ref 74).

are nonplanar structures in the ground state of uracil and adenine as discussed in Section 2. The vibrational frequency analysis was done for the low-lying excited states of these molecules, and the results are listed in the SI. For the excited states of uracil and adenine, the C_s structures obtained by imposing this symmetry group were also found to be saddle points. Based on the vibrational analysis, the $1B_{1g}$, $1B_{3g}$, $1A_u$, and $1B_{1u}$ states of *p*-benzoquinone were found to be local minima. The equilibrium structures of all these low-lying excited states have been calculated but for the $1A_g$ state. The O_1-C_2 bond elongation with respect to the ground state is large in the $1A_u$ and $1B_{1u}$ states (0.048 and 0.042 Å), and the C_3-C_4 bond length is significantly increased in the $1B_{1u}$ and $1B_{3g}$ states (0.040 and 0.066 Å). The C_2-C_3 bond contracts in all excited states, and the changes are large in the $1A_u$ and $1B_{3g}$ states. The deviations between PBE0 and SAC-CI are small for these excited states, and the rmsds are in the range 0.003−0.007 Å except for $1B_{1u}$.

For uracil, the structures of the $1A'$ and $1A''$ excited states have been calculated by restricting the C_{2v} structure as mentioned above. In the $1A'$ state, the changes in C_7-C_8 and C_8-C_2 bond lengths, with respect to the ground state, are significant, in particular at the SAC-CI level. The bond alternation occurs in the unit $C_7{=}C_8-C_2{=}O_1$. In the $1A''$ state, the excitation is also localized in the C_7-C_8-C_2-O_1 region: the C_2-O_1 (C_8-C_2) bond elongation (contraction) is large. The geometry changes in the third excited state, on the other hand, are distributed over the full molecule, which is symptomatic of a delocalized excitation. The rmsds between PBE0 and SAC-CI are large in uracil as a result of the larger geometrical changes estimated at the SAC-CI/D95(d,p) level.

Geometry optimizations of the $1A'$ and $1A''$ states for adenine were also performed imposing a C_s structure. These states are saddle points because of the planarity imposed on the amino group (see the SI). The geometry change in the $1A''$ state is significant, especially for the C_2-C_3 and N_8-C_9 distances, whereas the $1A'$ state variations are localized in the six membered ring. The rmsds between SAC-CI and TD-DFT are also relatively large: 0.010 and 0.022 Å in the $1A''$ and $1A'$ states, respectively.

The results of the equilibrium structures of 9,10-anthraquinone, coumarin, and 1,8-naphthalimide are summarized in Tables 7, 8, and 9, respectively. The frequency analyses of the stationary points demonstrate that among the excited states examined in Section 3.1, three excited states, namely, the $1A_{1g}$, $1A_u$, and $1B_{1u}$ states, are local minima in 9,10-anthraquinone, and the same holds for the $1A'$ state of coumarin and both the $1A_1$ and $1B_2$ states of 1,8-naphthalimide. Additionally, the equilibrium structures of the low-lying $1B_{1g}$, $1A_u$, and $1A_2$ excited states of 9,10-anthraquinone have been obtained with SAC-CI/D95(d,p). Among these states, the $1A_u$, and $1A_2$ states were found to be local minima, while the $1B_{1g}$ state was characterized as a saddle point. Based on the geometry changes in the B_{1g} and A_u states, the excitation is localized in the central benzoquinone unit for these states with large variations of the C−O and C_2-C_3 bond lengths. The geometry changes in the $1A_2$ state, on the other hand, are not so remarkable which indicates that the excitation is more delocalized. This is in agreement with the transition character and the analysis of the relevant MOs involved in the excitations. The rmsds between SAC-CI and TD-DFT for these bond lengths in D_{2h} structures were all below 0.007 Å.

In coumarin, the $1A'$ state which presents a large oscillator strength is a local C_s minimum, while the $1A''$ state has been found to be saddle point. In the $1A'$ state, the excitation is localized in the lactone unit, and the bond length changes are large for C_2-O_3, $C_{10}-C_{11}$, and C_2-C_{11}. As expected for a π-conjugated molecule, bond alternation occurs in this lactone unit. The same is true for the $1A''$ state, where the geometry change in O_1-C_2 and $C_{11}-C_2$ bond lengths is also remarkable. The deviation between the two methods is relatively large for the $1A'$ state: the computed rmsd was 0.024 Å.

Table 7. Geometrical Parameters (Å) and Vertical Emission Energies (Δ*E*, eV) Computed for the Valence Excited States for 9,10-Anthraquinone at the TD-PBE0/D95(d) and SAC-CI/D95(d,p) Levels

	ground	$1B_{1g}$		$1A_u$		$1A_2$	
	SAC	SAC-CI	PBE0	SAC-CI	PBE0	SAC-CI	PBE0
ΔE^a	-	2.84	2.80	2.87	2.85	2.56	2.70
O_1-C_2	1.221	1.259	1.254	1.270	1.266	1.229	1.283
C_2-C_3	1.497	1.473	1.461	1.463	1.450	1.486	1.444
$C_3.C_4$	1.403	1.415	1.410	1.414	1.410	1.407	1.415
C_4-C_5	1.390	1.383	1.385	1.385	1.386	1.387	1.384
C_5-C_6	1.403	1.412	1.411	1.409	1.409	1.409	1.409
C_6-C_7	1.390	1.383	1.385	1.385	1.386	1.385	1.388
C_7-C_8	1.403	1.415	1.410	1.414	1.410	1.418	1.404
C_8-C_3	1.401	1.399	1.408	1.417	1.430	1.406	1.414
rmsd[b]		0.006		0.007		0.025	

[a]Expt (ref 71, vapor): 2.95 eV. [b]rmsd between the PBE0 and SAC-CI bond lengths.

Table 8. Geometrical Parameters (Å) and Emission Energies (Δ*E*, eV) Computed for the Valence Excited States for Coumarin (TD-PBE0 and SAC-CI Levels)

	ground	1A′			1A″		
	SAC	SAC-CI	PBE0		SAC-CI	PBE0	
	D95(d,p)	D95(d,p)	D95(d)	6-311++G (2d,2p)	D95(d,p)	D95(d)	6-311++G (2d,2p)
ΔE^a	-	3.36	3.55	3.50	2.96	3.08	3.16
O_1-C_2	1.202	1.212	1.208	1.196	1.349	1.320	1.313
C_2-O_3	1.375	1.484	1.506	1.520	1.352	1.332	1.328
O_3-C_4	1.371	1.312	1.319	1.311	1.399	1.392	1.388
C_4-C_5	1.401	1.416	1.425	1.418	1.391	1.383	1.374
C_5-C_6	1.388	1.384	1.397	1.387	1.396	1.402	1.392
C_6-C_7	1.407	1.432	1.399	1.389	1.400	1.403	1.394
C_7-C_8	1.388	1.387	1.428	1.420	1.393	1.388	1.379
C_8-C_9	1.409	1.424	1.391	1.381	1.407	1.420	1.413
C_9-C_4	1.395	1.466	1.442	1.434	1.402	1.416	1.408
C_9-C_{10}	1.449	1.399	1.429	1.423	1.442	1.410	1.403
$C_{10}-C_{11}$	1.349	1.432	1.404	1.395	1.397	1.420	1.411
$C_{11}-C_2$	1.478	1.405	1.412	1.401	1.377	1.372	1.363
rmsd[b]		0.024			0.017		

[a]Expt (ref 69 and references therein, enol structure): 3.52, 3.28 eV. [b]rmsd between the PBE0 and SAC-CI bond lengths.

Table 9. TD-PBE0/D95(d) and SAC-CI/D95(d,p) Geometrical Parameters (Å) and Emission Energies (Δ*E*, eV) Computed for the Valence Excited States for 1,8-Naphthalimide

	ground	$1B_2$		$1A_1$	
	SAC	SAC-CI	PBE0	SAC-CI	PBE0
ΔE^a	-	3.67	3.97	3.42	3.45
N_1-C_2	1.395	1.395	1.390	1.394	1.388
C_2-O_3	1.211	1.217	1.228	1.228	1.230
C_2-C_4	1.493	1.479	1.467	1.46	1.466
C_4-C_5	1.378	1.404	1.399	1.445	1.431
C_5-C_6	1.415	1.422	1.424	1.373	1.381
C_6-C_7	1.378	1.403	1.397	1.429	1.420
C_7-C_8	1.423	1.414	1.413	1.409	1.414
C_8-C_9	1.425	1.493	1.478	1.441	1.429
C_4-C_9	1.421	1.415	1.421	1.409	1.415
rmsd[b]			0.012		0.008

[a]Expt (ref 64, in hexane): 3.30 eV. [b]rmsd between the PBE0 and SAC-CI bond lengths.

It should be noticed that for coumarins, the solvent effects change the symmetry of the first excited-states in TD-DFT and do influence significantly the CIS results as well, which could be a source of discrepancies.[76]

In 1,8-naphthalimide, the equilibrium structures of the $1A_1$ and $1B_2$ states are local minima, while other two states are saddle points. Both $1A_1$ and $1B_2$ states are dipole allowed, and the excitation is mostly localized on the naphthalene unit. The bond length changes in C_6-C_7 and C_8-C_9 are large in the $1B_2$ state, while the $1A_1$ state has large structure relaxation in C_4-C_5, C_5-C_6, and C_6-C_7. The rmsds between the two methods were of 0.012 and 0.008 Å for the $1B_2$ and $1A_1$ states, respectively.

In general, the SAC-CI and TD-DFT approaches give a qualitatively similar picture of the emitting states, although the discrepancies between the structures predicted by the two methods seems to be larger in the case of substantial localized relaxation of the excited states.

3.4. Effect of the Functional on Emission Energies.

Even if the PBE0 functional could be considered as a classical reference for TD-DFT calculations, several papers have underlined its breakdowns in the prediction of absorption and emission energies and the advantages provided by the most recent approaches.[34,35,37] Therefore, emission energies have been computed also with a selected number of functionals, and the obtained results are reported in Table 10 and in Figure 3.

dx.doi.org/10.1021/ct400097b | J. Chem. Theory Comput. 2013, 9, 2368−2379

Table 10. Emission Energies (eV) Calculated with Several Functionals Using the D95(d) Basis Set

molecule	state	SAC-CI	PBE0	CAM-B3LYP	B3LYP	M06	M06-2X	ωB97X-D
furan	$1B_2$	5.97	5.44	5.38	5.30	5.24	5.48	5.41
pyrrole	$1B_2$	6.12	5.80	5.73	5.65	5.53	5.83	5.76
pyridine	$1B_1$	4.12	3.97	4.09	3.89	3.81	3.84	4.08
p-benzoquinone	$1B_{1g}$	2.70	2.34	2.71	2.28	2.32	2.60	2.67
uracil	1A″	3.43	3.52	3.95	-	3.42	4.02	3.94
adenine	1A″	3.74	3.85	4.03	3.73	3.64	4.00	4.02
9,10-anthra-quinone	$1B_{1g}$	2.84	2.80	3.14	2.70	2.78	3.06	3.13
coumarin	1A′	3.36	3.55	3.81	3.29	3.49	3.82	3.82
1,8-naphthalimide	$1A_1$	3.42	3.45	3.60	-	3.36	3.63	3.62

These functionals have been chosen among those most widely used in chemistry (B3LYP, M06, and M06-2X) or belonging to the range-separated family, already known to provide good performances on exited states (CAM-B3LYP and ωB97X-D) with significant charge transfer character.[14] In order to have a straightforward comparison with the previous results only the D95(d) basis set has been considered.

The data collected in Figures 3 and 4 show reasonable agreement between SAC-CI and TD-DFT methods for all

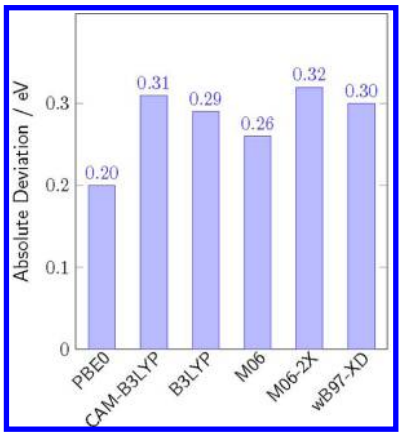

Figure 4. Effect of the functional on the absolute deviation of the first emission state with respect to the SAC-CI results, computed with D95(d) basis set.

functionals considered. In general, the TD-DFT emission energies are underestimated with respect to the SAC-CI values for small molecules, whereas those of two or three rings compounds are larger than the SAC-CI ones. This indicates that the TD-DFT error is not uniform for compounds of different size, a fact previously pointed out for absorption.[12] More in details, for the $1B_2$ state of furan, all functionals underestimate the emission energy by at least 0.49 eV (M06-2X) with a maximum of 0.73 eV (M06). For pyrrole, the underestimation for the $1B_2$ state is also large, and a better agreement was found for M06-2X (5.83 eV) and PBE0 (5.80 eV); these values should be compared with the 6.12 eV SAC-CI reference. For pyridine, the agreement between SAC-CI and TD-DFT is better than for furan and pyrrole, deviations being within about 0.3 eV. Indeed, CAM-B3LYP and ωB97X-D provide very close results, with errors as small as 0.03 and 0.04 eV, respectively. For these three molecules, PBE0 gave results relatively close to the SAC-CI ones; the differences are 0.15, 0.32, and 0.53 eV, respectively. For pyridine, among the TD-DFT methods, the PBE0 values are similar to those by CAM-B3LYP, M06-2X, and ωB97X-D.

Regarding the first excited state of *p*-benzoquinone, $1B_{1g}$, the CAM-B3LYP functional gives nearly the same result as SAC-CI, 2.71 eV. A negligible difference of 0.03 eV was also obtained with ωB97X-D. On the contrary, a severe underestimation occurs with B3LYP with a difference of 0.42 eV. For the emission energy of the 1A″ state of uracil, the agreement between the SAC-CI and TD-DFT values is also functional dependent. PBE0 and M06 give accurate values with the differences of 0.09 and 0.01 eV, respectively, compared to SAC-CI, while other functionals provide a large difference of ∼0.50 eV. For the 1A″ state of adenine, the best result was obtained using B3LYP with 0.01 eV of difference. The values obtained by PBE0 and M06 are close to each other with a difference found between 0.10 and 0.11 eV, while CAM-B3LYP, ωB97X-D, and M06-2X gave deviations of 0.26−0.29 eV. It is well-known that the latter three functionals provide very similar values for most transition energies.[80]

For the $^1B_{1g}$ state of 9,10-anthraquinone, the figures obtained with PBE0 (0.04 eV of difference), M06 (0.06 eV), and B3LYP (0.14 eV) are close to the SAC-CI value. On the contrary, the other functionals yield overestimation of the emission energy by at least 0.22 eV. For the 1A′ state of coumarin, most TD-DFT calculations overshoot the SAC-CI results at the exception of the B3LYP functional. Finally, for the $1A_1$ state of 1,8-naphtalamide, PBE0 allows us to obtain an excellent value of 3.45 eV (3.42 eV in SAC-CI), whereas M06 is also accurate, with a difference of 0.06 eV. All the other functionals, however, overestimate the emission energy by values ranging from 0.18 eV (CAM-B3LYP) to 0.21 eV (M06-2X). We failed to obtain the B3LYP values for uracil and 1,8-naphthalimide.

The benchmarking of methods for emission energies is tough because the results depend upon both the quality of the equilibrium geometries in the excited state and the associated transition energies. Looking at the total MADs, reported in Figure 4, obtained for the different functionals on the emission energy, one notices the good agreement between the PBE0 and SAC-CI results. Indeed, the averaged deviation of PBE0 is 0.20 eV and M06 yields a slightly larger error (0.26 eV), while other functionals providing larger deviations about 0.3 eV.

3.5. Effect of the Basis Set on TD-DFT Absorption and Emission. The last point to be assessed is the basis set dependence for absorption and emission energies as well as excited-state structures. In a previous detailed study on small organic molecules, it has been underlined that diffuse functions are necessary to obtain converged vertical absorption energy, and this has been then confirmed in several other studies.[17,47]

Among all considered molecules, pyrrole is showing the largest basis set dependence, as illustrated by Figure 5. The valence excited states, obtained with the PBE0 functional, are converged with the compact D95(d,p), 6-31G, and 6-31G(d,p)

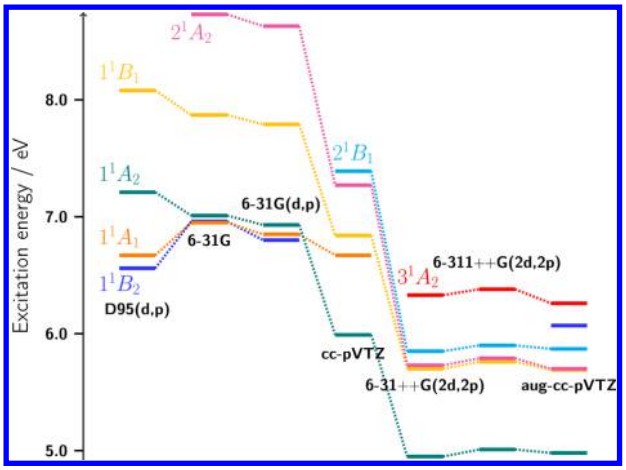

Figure 5. Basis set effects on the absorption energies for the lowest-lying excited states of pyrrole.

basis sets. Because the diffuse character is partly described by the outermost AOs in cc-pVTZ, the spectrum is intermediate with this basis set. Convergence of the transition energies for the Rydberg excited states is reached with the 6-31++G(2d,2p), 6-311++G(2d,2p), and *aug*-cc-pVTZ. Thus, special attention should be paid when calculating the excited states in these molecules where Rydberg states are below valence excited states.

The situation for the other molecules appears to be less problematic, since, generally speaking, the order of the electronic states is preserved when going from small to extended basis sets. In particular, the absorption energies of pyridine, *p*-benzoquinone, uracil, 9,10-anthraquinone, and coumarin will be addressed in the following. The excitation energies calculated by PBE0 with seven types of basis sets are summarized in the SI. For pyridine, the lowest four excited states have a valence character. The convergence is achieved with 6-311++G(2d,2p) and *aug*-cc-pVTZ, namely, the B_1, A_2, and A_1 states are located at 4.82, 5.19, and 6.30 eV above the ground state, respectively. The respective experimental values are 4.44, 4.99, and 6.38 eV. Concerning *p*-benzoquinone, the basis set dependence is also small, the difference of transition energies between small and big basis sets being within 0.03, 0.04, 0.07, and 0.08 eV for B_{1g}, A_u, B_{3g}, and B_{1u} states, respectively. The deviations from the experimental values are also very small as 0.06, 0.27, 0.15, and 0.12 eV for these states when using cc-pVTZ. For uracil, the comparison is done for the 1A′ state, for which the experimental value is 5.08 eV. For this state, the valence-Rydberg interaction seems to be relatively large, and the inclusion of diffuse or Rydberg function is required to guarantee the quality of the results. The convergence was obtained with the basis sets including diffuse functions, like the *aug*-cc-pVTZ (computed energy: 5.26 eV).

In the case of the B_{2u} state of 9,10-anthraquinone, the transition energies are within 0.1 eV for all basis sets. This indicates that the valence excited B_{2u} state is located far from Rydberg states and that interactions among these states are minor. For coumarin, the calculated values of the excitation energies, 4.28 and 4.74 eV, are still far from the experimental values, 3.99 and 4.53 eV, respectively. The excitation energies for the former (latter) state vary by 0.2 eV (0.1 eV) with the present sets of the basis sets. The excitation energies obtained using the 6-311++G(2d,2p) and *aug*-cc-pVTZ basis are very close, and the values are at convergence for these excited states.

For the lowest vertical emissions of all molecules, the convergence is already achieved with the smallest basis set

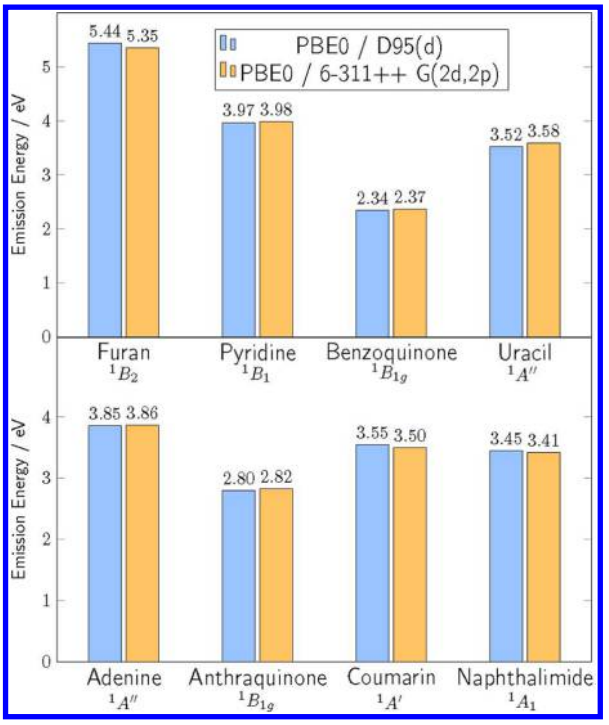

Figure 6. Basis set effects on emission energies computed at both PBE0/D95(d) and PBE0/6-311++G(2d,2p) levels.

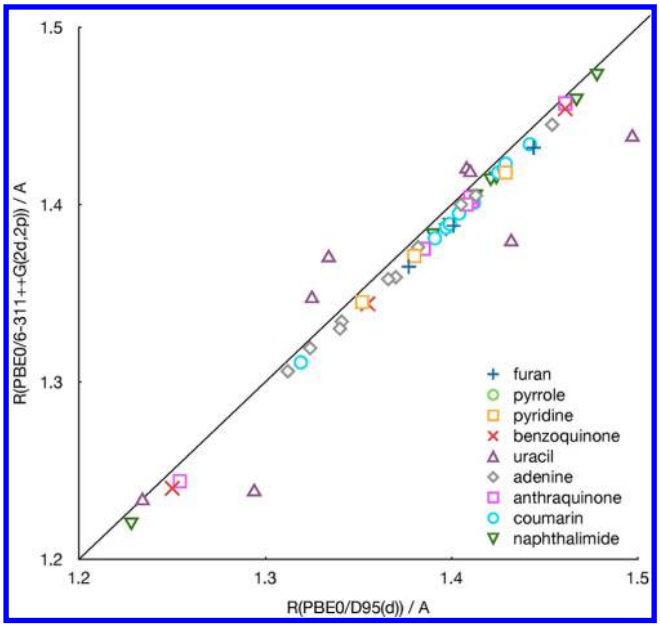

Figure 7. Selected excited-state bond lengths calculated with PBE0 using D95(d) and 6-311++G(2d,2p).

(D95(d)), making the analysis straightforward. Indeed, the average difference between the two basis sets is 0.04 eV (see Figure 6). The largest difference in energies between this basis and the largest 6-311++G(2d,2p) set is obtained for furan (0.09 eV), while changes as small as 0.01 eV are found for both adenine and pyridine.

The structures of the lowest excited states for all molecules, obtained with the D95(d) and the 6-311++G(2d,2p) basis sets, are collected in Tables 4−10. As clearly appears from these data and Figure 7, the reported bond lengths show a systematically

dx.doi.org/10.1021/ct400097b | J. Chem. Theory Comput. 2013, 9, 2368−2379

overestimation of about 0.010 Å when using the smallest basis set. It is noteworthy that all the functionals show a similar basis set dependence for both emission energies and structures.

Geometries of the two low-lying Rydberg excited states, namely $1A_2$ (3s) and $1B_1$ ($3p_y$) states, of furan and pyrrole were calculated by PBE0/6-311++G(2d,2p). Unlike valence excited states, the geometry changes of the Rydberg states are not so drastic, for example, −0.03, +0.03, and −0.07 Å, for O_1-C_2, C_2-C_3, and C_3-C_4 bonds, respectively, for the $1A_2$ (3s) state of furan. The optimized structures of the $1A_2$ and $1B_1$ states are similar in bond length. This is because the structures associated with Rydberg states reflect those of the corresponding ionized states, that are the π^{-1} states.

4. CONCLUSIONS

We have investigated the geometries of a panel of low-lying singlet excited states in nine π-conjugated heteroaromatic compounds by the direct SAC-CI and TD-DFT calculations. Indeed, the geometry relaxation in some $\pi\pi^*$ and $n\pi^*$ excited states of furan, pyrrole, pyridine, *p*-benzoquinone, uracil, adenine, 9,10-anthraquinone, coumarin, and 1,8-naphthalimide as well as their vertical transitions including Rydberg excited states have been analyzed in detail. The basis set and functional dependences of the results were also examined. The SAC-CI and TD-PBE0 calculations show reasonable agreement in both transition energies and excited-state equilibrium geometries of these π conjugated heteroaromatic compounds. The average difference in emission energies between SAC-CI and PBE0 was 0.20 eV for the lowest excited state in vertical transition for each molecule.

■ ASSOCIATED CONTENT

Ⓢ Supporting Information

Detailed SAC/SAC-CI results with Cartesian coordinates, CIS vibrational analyses, and detailed PBE0 results with several basis sets and functionals. This material is available free of charge via the Internet at http://pubs.acs.org.

■ AUTHOR INFORMATION

Corresponding Author

*E-mail: ehara@ims.ac.jp (M.E.), carlo-adamo@chimie-paristech.fr (C.A.).

Notes

The authors declare no competing financial interest.

■ ACKNOWLEDGMENTS

C.A. thanks Prof. Gerard Aka (ENSCP) for the organization of the joint ENSCP-IMS meeting, which is at the origin of the present work. M.E. and R.F. acknowledge the JST-CREST, a Grant-in-Aid for Scientific Research from the Japanese Society for the Promotion of Science (JSPS) and the Ministry of Education, Culture, Sports, Science, and Technology (MEXT) of Japan. D.J. acknowledges the European Research Council (ERC) and the *Région des Pays de la Loire* for financial support in the framework of a Starting Grant (Marches -278845) and a *recrutement sur poste stratégique*, respectively. The SAC-CI calculations were partly performed using the Research Center for Computational Science in Okazaki, Japan.

■ REFERENCES

(1) Nakatsuji, H.; Hirao, K. *J. Chem. Phys.* **1978**, *68*, 2053−2065.
(2) Nakatsuji, H. *Chem. Phys. Lett.* **1978**, *59*, 362−364.
(3) Nakatsuji, H. *Chem. Phys. Lett.* **1979**, *67*, 329−333.
(4) Mukherjee, D.; Mukherjee, P. K. *Chem. Phys.* **1979**, *39*, 325−335.
(5) Koch, H.; Jorgensen, P. *J. Chem. Phys.* **1990**, *93*, 3333−3344.
(6) Geertsen, J.; Rittby, M.; Bartlett, R. J. *Chem. Phys. Lett.* **1989**, *164*, 57−62.
(7) Stanton, J. F.; Bartlett, R. J. *J. Chem. Phys.* **1993**, *98*, 7029−7039.
(8) Peyerimhoff, S. D.; Buenker, R. J. *Adv. Quantum Chem.* **1975**, *9*, 69−104.
(9) Buenker, R. J.; Peyerimhoff, S. D. *Theor. Chim. Acta* **1968**, *12*, 183−199.
(10) Andersson, K.; Malmqvist, P.-A.; Roos, B. O.; Sadlej, A. J.; Wolinski, K. *J. Phys. Chem.* **1990**, *94*, 5483−5488.
(11) Hirao, K. *Chem. Phys. Lett.* **1992**, *190*, 374−380.
(12) Jacquemin, D.; Wathelet, V.; Perpète, E. A.; Adamo, C. *J. Chem. Theory Comput.* **2009**, *5*, 2420−2435.
(13) Jacquemin, D.; Perpète, E. A.; Ciofini, I.; Adamo, C.; Valero, R.; Zhao, Y.; Truhlar, D. G. *J. Chem. Theory Comput.* **2010**, *6*, 2071−2085.
(14) Peach, M. J. G.; Benfield, P.; Helgaker, T.; Tozer, D. J. *J. Chem. Phys.* **2008**, *128*, 044118.
(15) Stratmann, R. E.; Scuseria, G. E.; Frisch, M. J. *J. Chem. Phys.* **1998**, *109*, 8218−8224.
(16) Jacquemin, D.; Planchat, A.; Adamo, C.; Mennucci, B. *J. Chem. Theory Comput.* **2012**, *8*, 2359−2372.
(17) Goerigk, L.; Grimme, S. *J. Chem. Phys.* **2010**, *132*, 184103.
(18) Guido, C. A.; Jacquemin, D.; Adamo, C.; Mennucci, B. *J. Phys. Chem. A* **2010**, *114*, 13402−13410.
(19) Becke, A. D. *J. Chem. Phys.* **1993**, *98*, 5648−5652.
(20) Adamo, C.; Barone, V. *J. Chem. Phys.* **1998**, *108*, 664−675.
(21) Nakatsuji, H. *Acta Chim. Hung.* **1992**, *129*, 719−776.
(22) Ehara, M.; Hasegawa, J.; Nakatsuji, H. SAC-CI Method Applied to Molecular Spectroscopy. In *Theory and Applications of Computational Chemistry: The First 40 Years, A Vol. of Technical and Historical Perspectives*; Dykstra, C. E., Frenking, G., Kim, K. S., Scuseria, G. E., Eds.; Elsevier: Oxford, 2005; pp 1099−1141.
(23) Nakajima, T.; Nakatsuji, H. *Chem. Phys. Lett.* **1997**, *280*, 79−84.
(24) Nakajima, T.; Nakatsuji, H. *Chem. Phys.* **1999**, *242*, 177−193.
(25) Ishida, M.; Toyota, K.; Ehara, M.; Nakatsuji, H.; Frisch, M. J. *J. Chem. Phys.* **2004**, *120*, 2593−2605.
(26) Ehara, M.; Oyagi, F.; Abe, Y.; Fukuda, R.; Nakatsuji, H. *J. Chem. Phys.* **2011**, *135*, 044316.
(27) Nakatsuji, H. *Chem. Phys.* **1983**, *75*, 425−441.
(28) Fukuda, R.; Nakatsuji, H. *J. Chem. Phys.* **2008**, *128*, 094105.
(29) Frisch, M. J.; Trucks, G. W.; Schlegel, H. B.; Scuseria, G. E.; Robb, M. A.; Cheeseman, J. R.; Scalmani, G.; Barone, V.; Mennucci, B.; Petersson, G. A.; Nakatsuji, H.; Caricato, M.; Li, X.; Hratchian, H. P.; Izmaylov, A. F.; Bloino, J.; Zheng, G.; Sonnenberg, J. L.; Hada, M.; Ehara, M.; Toyota, K.; Fukuda, R.; Hasegawa, J.; Ishida, M.; Nakajima, T.; Honda, Y.; Kitao, O.; Nakai, H.; Vreven, T.; Montgomery, J. A., Jr.; Peralta, J. E.; Ogliaro, F.; Bearpark, M.; Heyd, J. J.; Brothers, E.; Kudin, K. N.; Staroverov, V. N.; Kobayashi, R.; Normand, J.; Raghavachari, K.; Rendell, A.; Burant, J. C.; Iyengar, S. S.; Tomasi, J.; Cossi, M.; Rega, N.; Millam, J. M.; Klene, M.; Knox, J. E.; Cross, J. B.; Bakken, V.; Adamo, C.; Jaramillo, J.; Gomperts, R.; Stratmann, R. E.; Yazyev, O.; Austin, A. J.; Cammi, R.; Pomelli, C.; Ochterski, J. W.; Martin, R. L.; Morokuma, K.; Zakrzewski, V. G.; Voth, G. A.; Salvador, P.; Dannenberg, J. J.; Dapprich, S.; Daniels, A. D.; Farkas, Ö.; Foresman, J. B.; Ortiz, J. V.; Cioslowski, J.; Fox, D. J. *Gaussian 09, Revision B.01*; Gaussian, Inc.: Wallingford, CT, 2010.
(30) Dunning, T. H., Jr. *J. Chem. Phys.* **1970**, *53*, 2823−2833.
(31) Krishnan, R.; Binkley, J. S.; Seeger, R.; Pople, J. A. *J. Chem. Phys.* **1980**, *72*, 650−654.
(32) Dunning, T. H., Jr.; Harrison, P. J. In *Modern Theoretical Chemistry*; Schaefer, H. F., III, Ed.; Plenum Press: New York, 1977; Vol. *2*, pp 1−28.
(33) Dunning, T. H., Jr. *J. Chem. Phys.* **1989**, *90*, 1007−1023.
(34) Yanai, T.; Tew, D. P.; Handy, N. C. *Chem. Phys. Lett.* **2004**, *91*, 51−57.
(35) Zhao, Y.; Truhlar, D. G. *Theor. Chem. Acc.* **2008**, *120*, 215−241.
(36) Zhao, Y.; Truhlar, D. G. *J. Phys. Chem.* **2006**, *110*, 5121−5129.

(37) Chai, J. D.; Head-Gordon, M. *Phys. Chem. Chem. Phys.* **2008**, *10*, 6615−6620.
(38) Nakatsuji, H.; Kitao, O.; Yonezawa, T. *J. Chem. Phys.* **1985**, *83*, 723−734.
(39) Serrano-Andres, L.; Merchan, M.; Nebot-Gil, I.; Roos, B. O.; Fulscher, M. *J. Am. Chem. Soc.* **1993**, *115*, 6184−6197.
(40) Palmer, M. H.; Walker, I. C.; Ballard, C. C.; Guest, M. F. *Chem. Phys.* **1995**, *192*, 111−125.
(41) Palmer, M. H.; Walker, I. C.; Guest, M. F. *Chem. Phys.* **1998**, *238*, 179−199.
(42) Nakano, H.; Tsuneda, T.; Hashimoto, T.; Hirao, K. *J. Chem. Phys.* **1996**, *104*, 2312−2320.
(43) Innes, K. K.; Ross, I. G.; Moomaw, W. R. *J. Mol. Spectrosc.* **1988**, *132*, 492−544.
(44) Walker, I. C.; Palmer, M. H.; Hopkirk, A. *Chem. Phys.* **1990**, *141*, 365−378.
(45) Wan, J.; Meller, J.; Hada, M.; Ehara, M.; Nakatsuji, H. *J. Chem. Phys.* **2000**, *113*, 7853−7866.
(46) Wan, J.; Hada, M.; Ehara, M.; Nakatsuji, H. *J. Chem. Phys.* **2001**, *114*, 5117−5123.
(47) Ciofini, I.; Adamo, C. *J. Phys. Chem. A* **2007**, *111*, 5549−5556.
(48) Bomble, Y. J.; Sattelmeyer, K. W.; Standon, J. F.; Gauss, J. *J. Chem. Phys.* **2004**, *121*, 5236−5240.
(49) Trommsdorff, H. P. *J. Chem. Phys.* **1972**, *56*, 5358−5372.
(50) Brint, P.; Connerade, J.-P.; Tsekeris, P.; Bolovinos, A.; Baig, A. *J. Chem. Soc., Faraday Trans. II* **1986**, *82*, 367−375.
(51) Goodman, J.; Brus, L. E. *J. Chem. Phys.* **1978**, *69*, 1604−1612.
(52) Meier, A. R.; Wagniere, G. H. *Chem. Phys.* **1987**, *113*, 287−307.
(53) Clark, L. B.; Peschel, G. G.; Tinoco, I., Jr. *J. Phys. Chem.* **1965**, *69*, 3615−3618.
(54) Mishra, S. K.; Shukla, M. K.; Mishra, P. C. *Spectrochim. Acta Part A* **2000**, *56*, 1355−1384.
(55) Pou-Amerigo, R.; Merchan, M.; Orti, E. *J. Chem. Phys.* **1999**, *110*, 9536−9546.
(56) Weber, J.; Malsch, K.; Hohlneicher, G. *Chem. Phys.* **2001**, *264*, 275−318.
(57) Honda, Y.; Hada, M.; Ehara, M.; Nakatsuji, H. *J. Phys. Chem. A* **2002**, *106*, 3838−3849.
(58) Epifanovsky, E.; Kowalski, K.; Fan, P.-D.; Valiev, M.; Matsika, S.; Krylov, A. I. *J. Phys. Chem. A* **2008**, *112*, 9983−9992.
(59) Silva-Junior, M. R.; Schreiber, M.; Sauer, S. P. A.; Thiel, W. *J. Chem. Phys.* **2008**, *129*, 104103.
(60) Santhosh, C.; Mishra, P. C. *J. Mol. Struct.* **1990**, *220*, 25−41.
(61) Callis, P. R. *Annu. Rev. Phys. Chem.* **1983**, *34*, 329−357.
(62) Myrvold, B. O.; Spanget-Larsen, J.; Thulstrup, E. W. *Chem. Phys.* **1986**, *104*, 305−313.
(63) Masrani, K. V.; Rama, H. S.; Bafna, S. L. *J. Appl. Chem. Biotechnol.* **1974**, *24*, 331−341.
(64) Wintgens, V.; Valat, P.; Kossanyi, J.; Biczok, L.; Demeter, A.; Berces, T. *J. Chem. Soc., Faraday Trans. II* **1994**, *90*, 411−421.
(65) Jacquemin, D.; Wathelet, V.; Preat, J.; Perpete, E. A. *Spectrochim. Acta, Part A* **2007**, *67*, 334−341.
(66) Preat, J.; Jacquemin, D.; Perpete, E. A. *Chem. Phys. Lett.* **2005**, *415*, 20−24.
(67) Jacquemin, D.; Perpete, E. A.; Scalmani, G.; Ciofini, I.; Peltier, C.; Adamo, C. *Chem. Phys.* **2010**, *372*, 61−66.
(68) Caricato, M.; Mennucci, B.; Tomasi, J.; Ingrosso, F.; Cammi, R.; Corni, S.; Scalmani, G. *J. Chem. Phys.* **2006**, *124*, 124520.
(69) Jacquemin, D.; Perpète, E. A.; Scalmani, G.; Frisch, M. J.; Assfeld, X.; Ciofini, I.; Adamo, C. *J. Chem. Phys.* **2006**, *125*, 164324.
(70) Jacquemin, D.; Adamo, C. *Int. J. Quantum Chem.* **2012**, *112*, 2135−2141.
(71) Itoh, T. *Chem. Rev.* **1995**, *95*, 2351−2368.
(72) Daniels, M.; Hanswirth, W. *Science* **1971**, *171*, 675−677.
(73) Gustavsson, T.; Banyasz, A.; Lazzarotto, E.; Markovitsi, D.; Scalmani, G.; Frisch, M. J.; Barone, V.; Improta, R. *J. Am. Chem. Soc.* **2005**, *128*, 607−619.
(74) Polewski, K.; Zinger, D.; Trunk, J.; Sutherland, J. C. *Radiat. Phys. Chem.* **2011**, *80*, 1092−1098.
(75) Silva-Junior, M. R.; Schreiber, M.; Sauer, S. P. A.; Thiel, W. *J. Chem. Phys.* **2010**, *133*, 174318.
(76) Jacquemin, D.; Perpeéte, E. A.; Assfeld, X.; Scalmani, G.; Frisch, M. J.; Adamo, C. *Chem. Phys. Lett.* **2007**, *438*, 208−212.
(77) Gromov, E. V.; Trofimov, A. B.; Vikovskaya, N. M.; Schirmer, J.; Koppel, H. *J. Chem. Phys.* **2003**, *119*, 737−753.
(78) Celani, P.; Werner, H.-J. *J. Chem. Phys.* **2003**, *119*, 5044−5057.
(79) Cai, Z.-L.; Reimers, J. R. *J. Phys. Chem. A* **2000**, *104*, 8389−8408.
(80) Jacquemin, D.; Perpète, E. A.; Ciofini, I.; Adamo, C. *Theor. Chem. Acc.* **2011**, *128*, 127−136.